



OPEN

SUBJECT AREAS:

CARBON NANOTUBES  
AND FULLERENES

ELECTRONIC MATERIALS

Received  
29 August 2013Accepted  
20 November 2013Published  
16 December 2013

Correspondence and requests for materials should be addressed to J.M.R. (jrazal@uow.edu.au) or G.G.W. (gwallace@uow.edu.au)

# Wet-spinning of PEDOT:PSS/ Functionalized-SWNTs Composite: a Facile Route Toward Production of Strong and Highly Conducting Multifunctional Fibers

Rouhollah Jalili, Joselito M. Razal &amp; Gordon G. Wallace

ARC Centre of Excellence for Electromaterials Science, Intelligent Polymer Research Institute, AIMM Facility, Innovation Campus, University of Wollongong, Wollongong, NSW 2522, Australia.

With the aim of fabricating multifunctional fibers with enhanced mechanical properties, electrical conductivity and electrochemical performance, we develop wet-spinning of composite formulation based on functionalized PEG-SWNT and PEDOT:PSS. The method of addition and loading are directly correlated to the quality and the ease of spinnability of the formulation and to the mechanical and electrical properties of the resultant fibers. Both the fiber modulus ( $Y$ ) and strength ( $\sigma$ ) scaled linearly with PEG-SWNT volume fraction ( $V_f$ ). A remarkable reinforcement rate of  $dY/dV_f = 417$  GPa and  $d\sigma/dV_f = 4$  GPa were obtained when PEG-SWNTs at  $V_f \leq 0.02$ . Further increase of PEG-SWNTs loading (i.e. up to  $V_f 0.12$ ) resulted in further enhancements up to 22.8 GPa and 254 MPa in Modulus and ultimate stress, respectively. We also show the enhancement of electrochemical supercapacitor performance of composite fibers. These outstanding mechanical, electrical and electrochemical performances place these fibers among the best performing multifunctional composite fibers.

Conducting polymers (CPs) are an intriguing class of conjugated polymers due to their inherent conductivity and the ability to induce dramatic changes in physical, mechanical and electrical properties by electrical signals<sup>1</sup>. Single walled carbon nanotubes (SWNTs) are also attractive as a result of their superior mechanical, electrical and electrochemical properties<sup>2,3</sup>. Many efforts have been made to combine CPs and SWNTs to integrate them into advanced multifunctional composites<sup>4-8</sup>. This kind of composite offers an attractive route to reinforce CPs while enhancing electrochemical performance based on morphological modification or electronic interaction between CPs and SWNTs<sup>5</sup>. It has been shown that composites based on CPs and SWNTs exhibit properties of each of the individual components with synergistic effect due to a facile charge transfer between the two constituents<sup>5</sup>. This charge transfer, which is in contrast with composites contained non-conducting matrix (i.e. PVA), prevents the enhanced contact resistance between adjacent tubes<sup>9</sup>. In the case of a non-conducting matrix, the efficiency of charge transfer within the adjacent SWNTs is strictly limited due to the insulator-coating of SWNTs<sup>9,10</sup>. Composite production using CPs eliminates this resistive barrier and maximizes the electron transport among SWNTs to improve the conductivity and electrochemical performance<sup>11</sup>. The addition of SWNTs to CPs is also valuable because of the limited conductivity of CPs in their reduced state; the state in which SWNTs can function as the conducting platform for charge delivery<sup>12</sup>.

Since composite production method determines the cost and performance of a final device, it is important to utilize a facile and scalable method to combine all of the necessary requirements for a practical multifunctional composite. To this end, fibers produced from CP-SWNTs not only can provide conductive and strong 3D framework for designing multifunctional architectures, but also are fully scalable for large-scale applications such as flexible and lightweight supercapacitors which can be further used in smart garments and electronic gadgets<sup>11-14</sup>.

One of the most successful methods used to fabricate CP based fibers is wet-spinning<sup>12,15-17</sup>. Using this method, the ability to exploit complementary properties of a CP along with the superlative mechanical, electrical and



electrochemical properties of SWNTs is also possible. Wet-spinning involves dispersing of SWNTs, with the aid of surfactant, then mixing with the CP dispersion at the required SWNTs loading followed by spinning of the dispersion into fibers<sup>11</sup>. However, this simple recipe presents several challenges: i) the presence of the surfactant or other dispersing agents can adversely affect mechanical properties of the composite. ii) The SWNT bundle size in the surfactant assisted dispersion is very concentration dependent<sup>11,18</sup>. iii) Quality high loading of SWNTs is still a strenuous task due to the formation of larger SWNTs bundles or aggregation at higher SWNTs loading<sup>11,19</sup>. iv) The electrical conductivity of the composites also suffers from either aggregation or discontinuous electrical connection due to the presence of the surfactant which is insulating and can have detrimental effects on the electrical contact between adjacent SWNTs<sup>9</sup>. These challenges can be overcome if a method to disperse SWNTs in a highly exfoliated state while maintaining this quality in the final CP-SWNTs formulation is developed and appropriate processing is utilized. Therefore, close-to-ideal composite fiber contains well-exfoliated SWNTs (without using dispersing agent) so that each tube is individually coated with a thin layer of CP. If this type of composite fiber is realized, not only mechanical properties of the CP are maximized, but also, SWNTs can provide a conduit to enhance charge delivery through the conducting fiber<sup>11</sup>.

Covalently functionalized SWNTs, such as polyethylene glycol functionalized SWNTs (PEG-SWNTs), provide high quality dispersion at high concentration ( $3.5 \text{ mg ml}^{-1}$ )<sup>20</sup> while omitting the need for the addition of any dispersing agents<sup>21</sup>. These advantages can be essentially used to provide homogenous composites with improved interfacial stress transfer between the SWNTs and polymer matrix thus maximizing the reinforcement of the composite<sup>22,23</sup>.

Among CPs, poly(3,4-ethylenedioxythiophene) poly(styrene sulfonate) (PEDOT:PSS) is one of the most commercially successful CPs which offers exciting opportunities for a wide range of applications such as supercapacitors, batteries, sensors, solar cells, transparent thin films, antistatic coating, composites and bionic devices<sup>24–28</sup>. This growing attention is due to the following characteristics: i) commercial availability with low price ( $\sim 6 \text{ EUR/g}$  for Orgacon<sup>TM</sup> Pellets), ii) processability in aqueous media, iii) response to electrical stimulation (conductivity, volume and colour changes), iv) the ability to be functionalized with biomolecules or nanomaterials, v) high ionic and electronic conductivity, vi) high environmental and thermal stability and vii) processability via commercially scalable methods such as wet-spinning and printing<sup>15–17,26–32</sup>.

With the aim to enhance mechanical properties, electrical conductivity and electrochemical performance of PEDOT:PSS fibers simultaneously, we hereby have investigated the effects of the addition of PEG-SWNTs and its loading on the resultant PEDOT:PSS/PEG-SWNTs fibers. We demonstrate that using PEG-SWNTs is the key to systematically control pre-formulated spinning solution to achieve higher loading while enhancing the properties to obtain multifunctional fibers. The method of addition of PEG-SWNTs to PEDOT:PSS and the loading are directly correlated to the quality and ease of spinnability of the formulation and to the mechanical and electrical properties of the resultant composite fibers. We also show the electrochemical performance of some selected fibers, which further demonstrates the unique advantages of employing PEG-SWNTs in PEDOT:PSS based fibers.

## Results

The spinning solution prepared by dissolving a required amount of PEDOT:PSS pellets to the PEG-SWNTs stock dispersion (Table S1). Wet-spinning of fibers containing PEDOT:PSS/PEG-SWNTs dispersions was performed using a non-solvent coagulation strategy to form fibers. Using PEG-SWNTs that are readily dispersible in water afforded good miscibility with PEDOT:PSS at all PEG-SWNTs loading. This compatibility also resulted in easy and

continuous wet-spinning of uniform composite fibers, regardless of the PEG-SWNTs loading. SEM images of the cross-sections of PEDOT:PSS/PEG-SWNTs fibers at various nanotube loadings, which fractured under tensile strain, are illustrated at Figure 1. The PEDOT:PSS/PEG-SWNTs fibers obtained were void-free with circular cross-section and diameter of 10 to 12  $\mu\text{m}$  irrespective of the PEG-SWNTs loading. Close inspection of the cross-section revealed only individual/small PEG-SWNTs bundles present in the fibers even at the highest PEG-SWNTs loading (0.12  $V_f$ ).

The cross-section of the pure PEDOT:PSS fiber differed from the composite fibers. Although the shape of the stress-strain curves were similar for all of the fibres, (Figure 2), the observed fibrillar morphologies of the fractured ends of PEDOT:PSS fibers suggest different failure mechanisms. For pure PEDOT:PSS fibers, the fibrillar morphologies characterized by the protruding short nodules are clear evidence of a plastic deformation of PEDOT:PSS during fracture. In contrast, some broken SWNTs that are observed in the composite fibers confirmed the contribution of PEG-SWNTs during load bearing. However, some micron-lengths of PEG-SWNTs which protruded from the broken ends, especially at higher loadings, revealed that some of the fractures occurred at the PEDOT:PSS/PEG-SWNTs interface. Nanotube pull-out, at higher loading, suggests nanotube slippage at the SWNT-SWNT interface at the PEG-SWNTs bundles (aggregate) and non-ideal interfacial stress transfer due to the lack of a thick polymer coating on the PEG-SWNTs<sup>19</sup>.

Significant reinforcing effect of PEG-SWNTs are illustrated in the stress-strain curves of the PEDOT:PSS/PEG-SWNTs composite fibers at various PEG-SWNTs loading (Figure 2). Both strength and modulus increased as the volume fraction of PEG-SWNTs increased. We have measured Young's modulus,  $Y$ , ultimate tensile strength,  $\sigma$ , strain at break,  $\epsilon$ , and toughness,  $T$ , as a function of nanotube volume fraction from stress strain curves as shown in Figure 3. The highest enhancement in the modulus of fibers (seven-fold enhancement) achieved at the highest nanotube loading (22.8 GPa at 0.12  $V_f$ ). However, at low PEG-SWNTs loadings

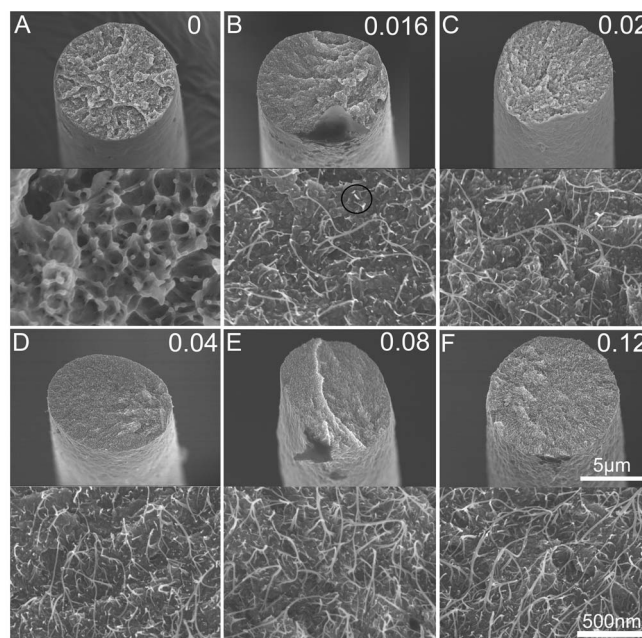


**Figure 1** | SEM images of the cross-sections of PEDOT:PSS/PEG-SWNTs composite fibers broken under tensile strain at low and high magnifications showing shape and microstructure of PEDOT:PSS/PEG-SWNTs composite fiber at various PEG-SWNTs loadings. Volume fraction of PEG-SWNTs indicated at each pair images. Circle at B shows broken ends of PEG-SWNTs.

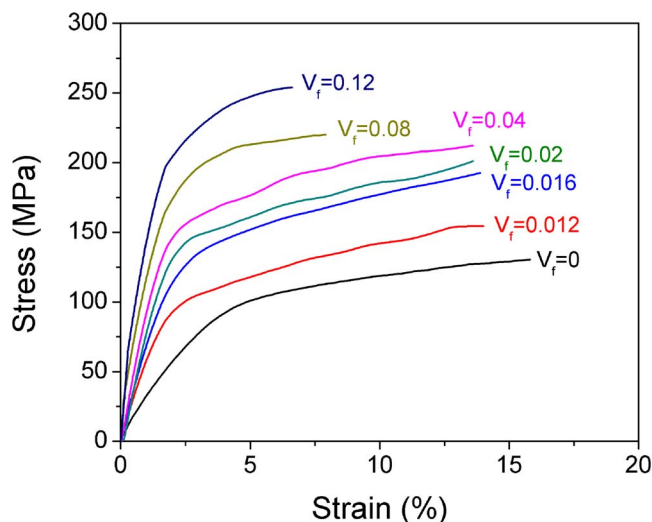


**Figure 2** | Representative stress-strain curves of PEDOT:PSS/PEG-SWNTs composite fibers at various nanotube loadings (represented by the numbers next to the curves, in volume fraction).

( $\leq 0.02 V_f$ ) the reinforcement was more striking and all of the moduli were above the theoretically calculated modulus of composite fiber with randomly orientated filler. The rule of mixtures predicts the composite modulus by<sup>33</sup>:

$$Y = (\eta_l \eta_o Y_{\text{SWNT}} - Y_m) V_f(\text{SWNT}) + Y_m \approx \eta_l \eta_o Y_{\text{SWNT}} V_f(\text{SWNT}) \quad (1)$$

Where  $\eta_l$  is the length efficiency factor (related to the aspect ratio),  $\eta_o$  is the orientation efficiency factor which is 0.2 and 1 for randomly oriented and perfectly oriented, respectively.  $Y_{\text{SWNT}}$  and  $Y_m$  are the SWNT and polymer modulus, respectively. In this model, a linear increase of modulus with  $V_f$  is predicted. The approximation used in Equation 1 is valid when the contribution of the filler to the fiber modulus is much larger than the polymer-only modulus, which is the case for our fibers. The slope of the linear region ( $dY/dV_f$ ) has been measured based on the data presented on Figure 3A to evaluate the degree of reinforcement<sup>19,23,33,34</sup>.

The data from Figure 3 clearly indicate that reinforcement occurred at two distinct regions (below and above PEG-SWNTs loading of  $0.02 V_f$ , referred to as regions I and II, respectively). In region I, PEG-SWNTs  $\leq 0.02$ , the  $dY/dV_f$  was 417 GPa. This reinforcement rate is found to be significantly higher than for the highest reported for PVA/SWNTs fibers (i.e. 254 GPa for SWNTs  $\leq 0.1 V_f$ ) and surfactant assisted PEDOT:PSS/SWNTs fibers (i.e. 80 GPa for SWNTs  $> 0.02 V_f$ )<sup>11,19</sup>. Other SWNTs/PVA based fibers also presented much lower  $dY/dV_f$  of around 125 GPa due to lower efficiency of SWNTs at high loading (based on 2 volume fractions, 0 and 0.6)<sup>35</sup>. The highest  $dY/dV_f$  of 449 GPa was reported for dry-jet wet-spun fibers of Poly(*p*-phenylene benzobisoxazole)/SWNTs liquid crystals (data obtained from only two volume fractions)<sup>36</sup>, owing to the extremely high modulus of the host polymer (138 GPa) and self-orientation properties of liquid crystals. Next high value was obtained from the gel-spinning of organic solvent based PVA-SWNTs ( $dY/dV_f = 406$  GPa)<sup>37</sup>. Other CNT based wet-spun fibers calculated by Wang et al<sup>36</sup>. had  $dY/dV_f$  values around 150 GPa. Comparing the data presented in the literature (some of them mentioned) with the reinforcement rate obtained for the current PEDOT:PSS/PEG-SWNTs fibers, it is clear that the PEG-functionalized SWNTs have a remarkable reinforcement effect even at low SWNT loading.

The  $dY/dV_f$  decreased to 108 GPa at region II and is attributed to the observed PEG-SWNTs bundling at high PEG-SWNTs loading (Figure 1). This result is in accordance with equation 1 i.e. if PEG-SWNTs bundle size is doubled (aspect ratio is halved) and keeping all

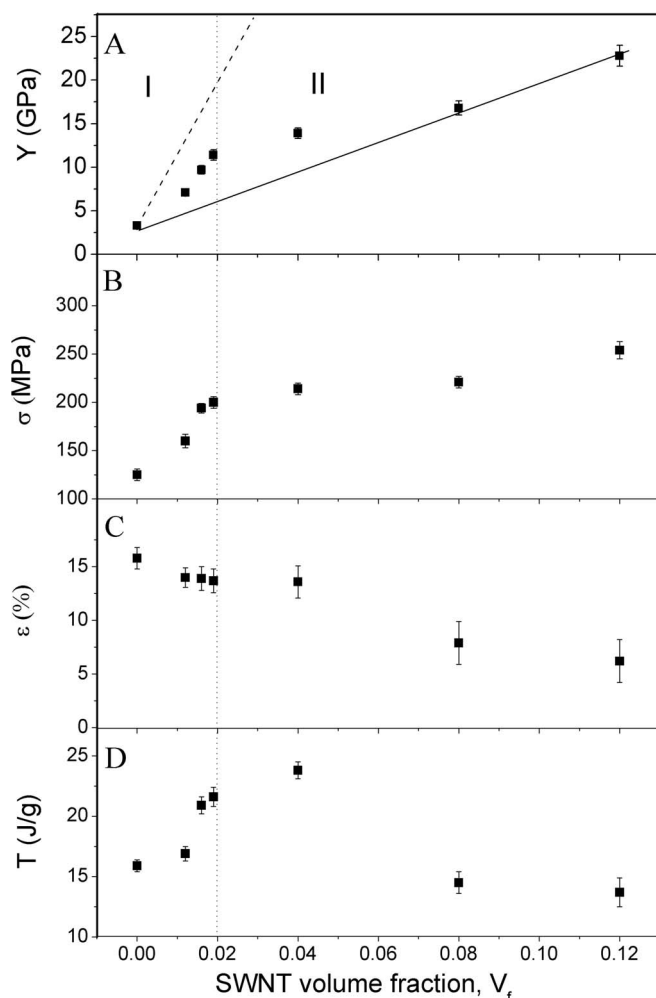


**Figure 3** | Comparison of the mechanical properties of PEDOT:PSS/PEG-SWNTs composite fibers as a function of PEG-SWNTs loading. Lines drawn in A are the theoretical reinforcement for perfectly aligned (dashed) and randomly oriented (solid) PEDOT:PSS/PEG-SWNTs fiber.

the other parameters the same, then modulus will decrease by 20%. Moreover, due to the presence of SWNT bundles, it can be expected that these modulus values could further decrease due to interfacial slippage.

In order to compare the stress transfer between the PEDOT:PSS matrix and PEG-SWNTs in the first and second region, Raman spectroscopy was carried out. It has been found that as the composite fiber is strained, the position of the  $G'$  band of PEG-SWNTs ( $2647 \text{ cm}^{-1}$ ) tend to shift linearly with deformation rate (strain)<sup>38</sup>. By monitoring the  $G'$  band shifts in the composite fibers under an applied strain (0.5%), the effectiveness of the stress transfer between PEDOT:PSS and PEG-SWNTs was evaluated. The measured shift in the first region ( $8 \text{ cm}^{-1}$  for PEG-SWNTs  $0.02 V_f$ ) was four times higher than the second region ( $2 \text{ cm}^{-1}$  for PEG-SWNTs  $0.12 V_f$ ). This four factor difference was well correlated by the  $dY/dV_f$  values in both regions ( $417 \text{ GPa}/108 \text{ GPa} \approx 4$ ); illustrating consistency in the mechanical measurements and Raman observations.

The reinforcement in strength also occurred at the two distinct PEG-SWNTs loading regions observed for modulus (Figure 3B). In region I, the tensile strength peaked at  $\sim 201$  MPa and the degree of reinforcement ( $d\sigma/dV_f$ ) was 4.0 GPa which was significantly higher than the highest reported for PVA/SWNTs fibers (2.8 GPa) and surfactant assisted PEDOT:PSS/SWNTs fibers (3.2 GPa for  $0.02 V_f$ )<sup>11,19</sup>. This substantial increase in tensile strength of the fibers



reflects that the quality of dispersed PEG-SWNTs is maintained in the bulk fibers even after the composite formulation and wet-spinning processes. It also reflects the enhanced compatibility of PEDOT:PSS with the type of CNT used. The PEG functionalities affords great miscibility with PEDOT:PSS, which resulted in sustained efficient reinforcement even at high PEG-SWNTs loading. In region II, further addition of PEG-SWNTs increased the strength of fibers up to 254 MPa at  $d\sigma/dV_f = 0.5$  GPa. This enhancement is in contrast with our previous report on surfactant assisted SWNTs/PEDOT:PSS composite when increasing of SWNTs significantly reduced the mechanical properties of composite fibers<sup>11</sup>.

Another measure of a good reinforced composite is toughness (the total energy required to break the fiber composite), which is dependent on both strength and breaking strain of the material. The change in toughness of the composite fibers followed the same trend as modulus and strength even when breaking strain decreased with PEG-SWNTs loading. The highest toughness was measured at PEG-SWNTs loading of 0.04  $V_f$  (23.8 J g<sup>-1</sup>) and is ~70% higher than the pure PEDOT:PSS fiber (15.9 J g<sup>-1</sup>). Beyond this PEG-SWNTs loading, the toughness decreased with strain. SEM studies showed (Figure 1) PEG-SWNTs bundles were slightly bigger and much closer together compare to those observed in fibers containing PEG-SWNTs  $V_f \leq 0.02$ . At low volume fractions the higher effective reinforcing surface area of the individual/small PEG-SWNTs bundles led to better mechanical properties, compared to when larger PEG-SWNTs bundles are used. It has also been found that slightly larger PEG-SWNTs bundles at high PEG-SWNTs loadings formed stress-concentration points and defect sites along the fiber length which adversely affected breaking strains and toughness.

Shown in Figure 4 are the measured electrical conductivities of as-prepared and secondary doped<sup>15</sup> composite fibers. Similar to mechanical properties, the electrical conductivities were found to be dependent on PEG-SWNTs loading. At the highest loading (0.04  $V_f$ ), composite fibers displayed a three-fold increase in conductivity at the rate of  $dS/dV_f = 200$  S cm<sup>-1</sup>. Note that the measured conductivity values represent the increase in conductivity contributed solely by the addition of PEG-SWNTs. Further conductivity enhancement was achieved *via* secondary doping of PEDOT:PSS through post-spinning treatment with ethylene glycol (EG). All secondary doped fibers displayed enhanced conductivities, albeit at varying degrees. The highest conductivity of ~400 S cm<sup>-1</sup> was achieved at a PEG-SWNTs loading of 0.016  $V_f$  ( $dS/dV_f = 2788$  S cm<sup>-1</sup>), which is comparable with SWNTs/PEDOT:PSS fibers processed using surfactant<sup>11</sup>. However, the mechanical properties are not sacrificed due to the elimination of the surfactant. This conductivity also was higher than the CNT based fibers reported by Barisci et al<sup>39</sup>, and Kozlov et al<sup>40</sup>, who achieved electrical conductivities up to 167 S cm<sup>-1</sup> after annealing CNT fibers at high temperatures. The measured conductivity compared favorably with values for the pure CNT-twisted yarns reported by M. Zhang et al. (ca. 300 S cm<sup>-1</sup>)<sup>41</sup> and X. Zhang et al. (ca. 410 S cm<sup>-1</sup>)<sup>42</sup>. It is noteworthy that most of the highly conducting SWNT-based composite fibers can achieve high conductivity when filled with at least 50 wt% SWNTs. For example, the electrical conductivity of PEDOT:PSS/PEG-SWNTs fibers (~400 S cm<sup>-1</sup>) was close to HA-CNT composite fibers (66 to 537 S cm<sup>-1</sup> depending on the coagulation strategy), while the latter contained much higher SWNTs loading (~2 wt% vs. ~67 wt%, respectively)<sup>43</sup>. The addition of much lower amounts of PEG-SWNTs, while obtaining the highest level of conductivity, make wet-spinning of PEDOT:PSS/PEG-SWNTs fibers an economical and viable choice.

Unexpectedly, further increase in the PEG-SWNTs loading up to 0.12  $V_f$  resulted in a decrease in conductivity of the fiber to ~200 S cm<sup>-1</sup>. The conductivity enhancement in secondary doped PEDOT:PSS fibers was previously associated with the conformational transformations and molecular ordering of PEDOT:PSS chains as a

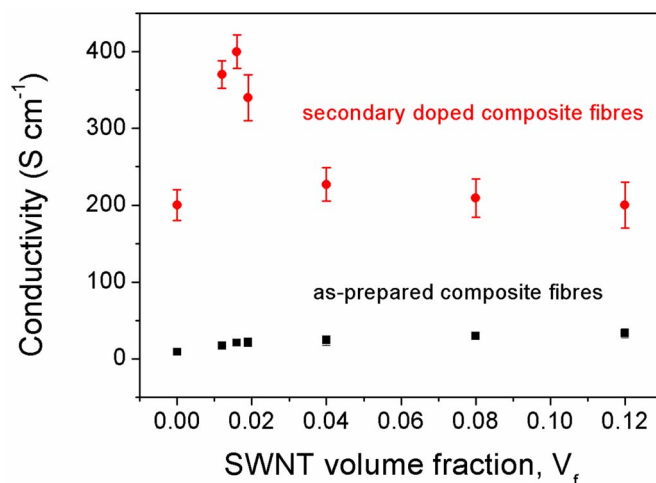


**Figure 4** | Comparison of the electrical properties of as-prepared and secondary doped composite fibers as a function of PEG-SWNTs loading.

consequence of phase segregation between PEDOT and PSS segments<sup>15</sup>. For the fibers presented here, it is reasoned that the higher modulus of composite fibers possibly limits these conformational changes, hence lower conductivity is observed in composite fibers with higher modulus. This effect is magnified at high PEG-SWNT loadings where the differences in modulus and strength between pure PEDOT:PSS and composites became much more significant (Figure 3).

The positive effect of the secondary doping was not limited to electrical conductivity; it also resulted in an enhancement in the final mechanical properties of the fibers. Figure 5 shows stress-strain curves of the secondary doped composite fibers as a function of PEG-SWNTs loading. The highest loading, the tensile strength and modulus increased from  $254 \pm 9$  MPa and  $22.8 \pm 1.2$  GPa to  $282 \pm 6$  MPa and  $25.0 \pm 1$  GPa, respectively. After phase separation between PEDOT segments and PSS due to the screening effect of the secondary doping, enhanced connection between PEDOT chains improved both the electrical and mechanical properties of the composite fibers.

The electrochemical behavior of the secondary doped composite fibers was investigated using cyclic voltammetry. This study evaluates the additional benefits gained from using PEG-SWNTs as mechanical and electrical reinforcing agents. Both three-electrode and two-electrode (symmetric) cells were used; the latter test configuration is valuable in estimating the capacitance of the fibers when used as electrode(s) in an electrochemical supercapacitor device. For these experiments two PEG-SWNTs loadings of 0.02 and 0.12  $V_f$  were compared. These PEG-SWNTs loadings were chosen due to the distinct transitions and differences in mechanical and electrical properties that were observed.

The more clearly defined redox peaks in the CV relates to the enhanced conductivity of PEDOT:PSS fiber after PEG-SWNTs addition. Also evident is the increased specific current response and the well-defined rectangular-shape of the cyclic voltammograms indicative of highly capacitive behaviour.

In a two-electrode configuration (Figure 6B), the capacitive behavior of all fibers was represented by the near-rectangular shaped CVs at scan rates of 50 mV s<sup>-1</sup>. Significant differences in the specific capacitances that were dependent on the PEG-SWNTs loading were observed. In comparison with the specific capacitance (two-electrode cell) of pure PEDOT:PSS fiber (10 F g<sup>-1</sup>), the highest PEG-SWNTs loading resulted in an approximately two-fold (22 F g<sup>-1</sup>) increase in specific capacitance for composite fibers.

The near-rectangular shape of the CVs obtained from the two-electrode configuration suggests that the overall internal resistance is

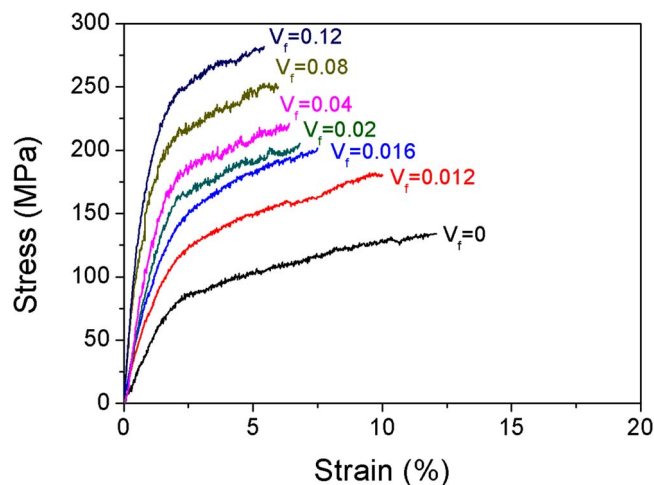


**Figure 5** | Representative stress-strain curves of secondary doped PEDOT:PSS/PEG-SWNTs composite fibers at various nanotube loadings (represented by the numbers next to the curves, in volume fraction).

low, owing to the improved fiber conductivity *via* PEG-SWNTs addition. The observed dependence of specific capacitance on CNT loading was due to the increased electroactive surface area arising from the combination of micro- and nano-porosity of composite fibers, and their inherent high conductivity. The open mesoporous network of PEG-SWNTs allows for an easy access of ions to the electrode/electrolyte interface and a more effective contribution of the pseudo-faradaic properties of PEDOT. The introduction of PEG-SWNTs into PEDOT:PSS matrix improves the electrical conductivity and mechanical properties while providing an additional active material for capacitive energy storage. Comparison of the specific capacitance of our composite fibers with those reported for PEDOT:PSS/SWNTs<sup>7,44,45</sup> and pure CNT fibers<sup>40</sup> in the literature reveals a similar performance achieved by our composite fibers that only required much lower CNT loadings. This higher efficiency was as a result of the high surface area of composite fibers and easier access of the ions to the individual/small bundles of CNTs dispersed in the polymer matrix promoting good wettability of the fiber by the electrolyte.

The use of PEG-SWNTs additive provided further benefit by improving the durability of the fiber electrode during repeated cycling. Notably, extended cycling (up to 500 cycles for composite fibers) revealed higher capacitance retention from the composite fibers irrespective of PEG-SWNTs loading compared with pure PEDOT:PSS fibers (Table 1). The stability of the enhanced ionic and electronic transport of the composite fibers depicts a strong interaction between the aromatic CNTs and the  $\pi$ -conjugated PEDOT:PSS polymer chains.

## Discussion

Utilizing functionalized SWNTs in the wet-spinning approach eliminated the use of dispersing agents to stabilize the SWNTs in the spinning solution. This, in turn, resulted in achieving fibers with superior physical and mechanical properties eliminating the adverse

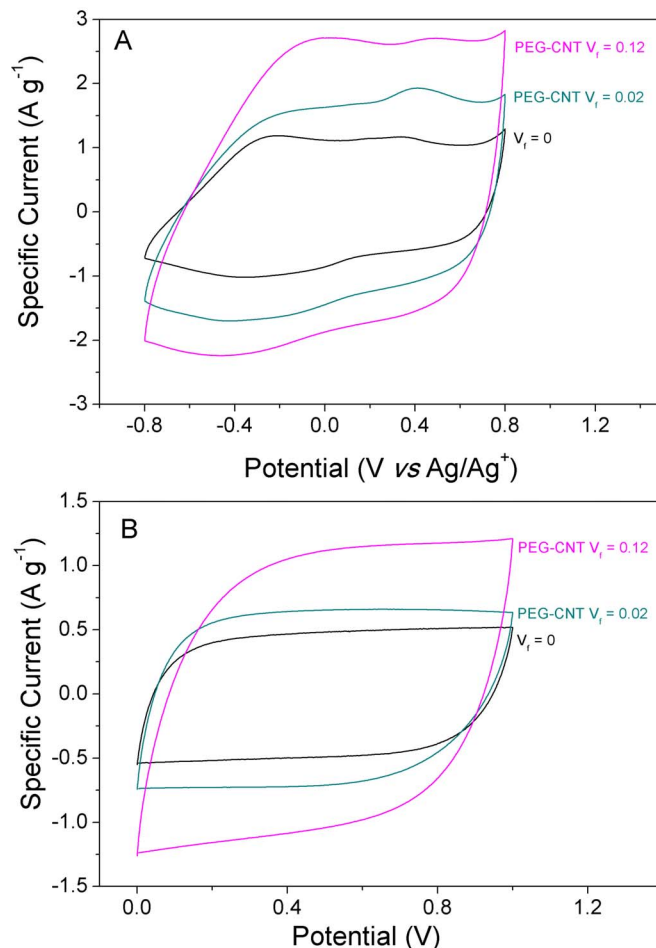


**Figure 6** | CV of PEDOT:PSS/PEG-SWNTs composite fibers as a function of  $V_f$  in 0.1 M TBABF<sub>4</sub>/acetonitrile taken at a scan rate of 50 mV s<sup>-1</sup>. (A) three-electrode cell system when potential measured vs Ag/AgNO<sub>3</sub>. (B) two-electrode (symmetric) cell.

effects of dispersing agents<sup>11</sup>. Excluding PVA from the coagulation bath<sup>35</sup> also avoided its adverse effect on the electrical properties which resulted in highly conducting fibers.

Maximizing the volume fraction of SWNTs was a challenge as a certain amount of PEDOT:PSS in the spinning formulation was required to make the dispersion spinnable. The role of PEDOT:PSS in the spinning solution is to increase viscosity of the solution and consequently provide spinnability. Direct blending of the highest achievable concentration of homogenous dispersions of PEDOT:PSS (25–30 mg ml<sup>-1</sup>) and PEG-SWNTs (3.2 mg ml<sup>-1</sup>) have limited the PEG-SWNTs  $V_f$  to 0.06 due to the excess amount of water which utilized to disperse PEDOT:PSS. This challenge has been addressed by the gradual addition of PEDOT:PSS pellets to the PEG-SWNTs stock dispersions, while the solution was being mixed by homogenizer, provided a homogenous dispersion without the need for excess water. In this method, it was possible to systematically control the

**Table 1** | Summary of the electrochemical performance of PEDOT:PSS/PEG-SWNT composite fibres

Fibre type	CNT loading ( $V_f$ )	Specific capacitance (F g <sup>-1</sup> )		
		3 electrode	2 electrode	Capacitance retention after 500 cycles (%)
PEDOT:PSS	0	15	10	86.7
PEDOT:PSS/PEG-SWNT	0.02	26	14	91.3
PEDOT:PSS/PEG-SWNT	0.12	35	22	91.5



loading of PEDOT:PSS in the spinning formulation as well as achieving higher volume fraction of nanotubes in the final fibers ( $V_f = 0.12$ , Table S1). Therefore, precise control of SWNTs loading in the spinning solution and hence a systematic parametric study of the reinforcement effect of SWNTs were possible due to the fact that there were only PEG-SWNTs and polymer in the spinning solution and the resultant fibres.

The other advantage of using functionalized PEG-SWNTs over the surfactant stabilized SWNT was that the dispersion was not sensitive to the amount of water which was added to the solution whereas addition of water to the surfactant stabilized formulation causes segregation of PEDOT:PSS and SWNTs<sup>11</sup>. Moreover, It has not been possible to use homogenizer to make very uniform PEDOT:PSS/surfactant stabilized-SWNTs due to extensive formation of foam and consequently crashing out of the SWNTs from the dispersion. Heterogeneous mixture of previously described surfactant assisted SWNTs and PEDOT:PSS has been resulted in non-uniform stress distribution and the presence of stress-concentration regions which has been shown to lead to early fracture of fiber<sup>11</sup>. In our case, the PEG functionality affords great miscibility with PEDOT:PSS, which ensued a homogenous composite fibers of isolated tubes coated with a layer of polymer, and located in close proximity to another. Moreover, axial tensions during the wet-spinning process has provided some alignment of the tubes in the direction of the fiber axis (Raman study, Figure S1), even at high PEG-SWNTs loading. Such a structure is prerequisite to efficient load transfer within the polymer-nanotube network.

We believe that the methods and results presented here will provide useful strategies in solving the fundamental challenges that hampered the progress in processing CP-based composite fibers. The present approach to fabricate fibers from PEDOT:PSS and functionalized SWNTs is sufficiently general to open the way to a broad range of CPs for possible applications in different fields. These fibers offer exciting opportunities for the development of intriguing macroscopic architectures for possible application in a wide range of areas such as energy storage, sensors and microelectrodes.

## Methods

**Materials.** The materials used in this work were all sourced commercially and used as received. PEDOT:PSS pellets were from Agfa under the trade name Orgacon dry (Lot. #A62 0000AC), and polyethylene glycol-functionalized SWNTs (PEG-SWNTs) were from Carbon Solutions (Lot. 07- 180).

**Preparation of spinning solutions.** PEG-SWNTs stock dispersions (at 5 mg ml<sup>-1</sup>) were prepared directly by adding 50 mg of PEG-SWNTs to 10 ml Milli-Q water (no additional surfactant is used). These PEG-SWNTs stock dispersions were subjected to 30 min of high-power tip sonication (SONICS Vibra Cell 500 W, 30% amplitude) followed by a 1 hr low-power bath sonication (Branson B5500R-DTH) and then subjected to another 30 min of high-power tip sonication before being allowed to rest overnight. Centrifugation (eppendorf 5702) of the stock dispersions was carried out at 4400 rpm (3000 g) for 90 min and the supernatant carefully decanted and saved. The post-centrifuge PEG-SWNTs of 3.2 mg ml<sup>-1</sup> was concentration determined from absorbance measurements at 660 nm<sup>20</sup>. All PEDOT:PSS/PEG-SWNTs composite wet-spinning formulations were then subsequently prepared by adding the required amount of PEDOT:PSS pellets to the above PEG-SWNTs stock dispersion to achieve formulations with PEDOT:PSS concentrations between 10 to 20 mg ml<sup>-1</sup> and PEG-SWNTs volume fraction ( $V_f$ ) of up to 0.12 (Table S1). The spinning formulations were further homogenized at 18,000 rpm for 10 min followed by 1 hr bath sonication prior to using in wet-spinning experiments.

**Fiber spinning.** The PEDOT:PSS/PEG-SWNTs composite fibers were fabricated at room temperature using a previously described wet-spinning technique that involves the use of non-solvent coagulation strategy with the spinning solution being injected from top to bottom of the coagulation bath<sup>11,15</sup>. Typically, about 5 ml of the spinning formulation in a syringe was extruded through a 20 gauge blunt needle (as a spinneret) into a coagulation bath (isopropanol) controlled by a syringe pump at flow rates between 0.8 to 2 mg hr<sup>-1</sup>. Fibers collected at the bottom of the coagulation bath were wound continuously onto a winding spool at a constant speed of 4 m min<sup>-1</sup>. In evaluating the effects of post-spinning treatment using ethylene glycol (EG), the as-spun fibers were wetted with (EG) by immersing them for 5 minutes and then oven drying at 150°C for 30 min while the fibers were under tension.

**Characterization.** The mechanical properties of the fibers were measured using a Shimadzu tensile tester (EZ-S) at a strain rate of 0.5% min<sup>-1</sup>. Samples were mounted on aperture cards (1 cm length window) with commercial superglue and allowed to air dry. Young's modulus ( $Y$ ), tensile strength ( $\sigma$ ), breaking strain ( $\epsilon$ ), and breaking energy (toughness) were calculated and the mean and standard deviation reported ( $n = 10$ ). A linear four-point probe conductivity cell with uniform 2.3 mm probe spacing was employed to measure the conductivity of the fibers (under laboratory humidity and temperature conditions) using a galvanostat current source (Princeton Applied Research Model 363) and a digital multimeter (HP Agilent 34401A). Electrochemical behaviour of the PEDOT:PSS/PEG-SWNTs composite fibers in deoxygenated organic electrolyte (0.1 M tetrabutylammonium tetrafluoroborate in acetonitrile) was investigated via CV using a potentiostat/galvanostat (Princeton Applied Research Model 363). A three-electrode cell constitutes of a free standing composite fiber working electrode, an Ag/AgNO<sub>3</sub> reference electrode and a platinum mesh auxiliary electrode (potential window from -0.8 V to 0.8 V). A symmetrical two electrode configuration constitutes of free standing composite fibers as cathode and anode (potential window from 0 V to 1 V).

1. Skotheim, T. A. & Reynolds, J. *Conjugated Polymers: Processing and Applications*. Third Edition edn, Vol. 1 (CRC Press, 2006).
2. Yu, M.-F., Files, B. S., Arepalli, S. & Ruoff, R. S. Tensile Loading of Ropes of Single Wall Carbon Nanotubes and their Mechanical Properties. *Phys. Rev. Lett.* **84**, 5552–5555 (2000).
3. Yu, M.-F. *et al.* Strength and Breaking Mechanism of Multiwalled Carbon Nanotubes Under Tensile Load. *Science* **287**, 637–640 (2000).
4. Baibarac, M., Baltog, I. & Lefrant, S. in *Nanostructured Conductive Polymers* 209–260 (John Wiley & Sons, Ltd, 2010).
5. Baibarac, M. & mez-Romero, P. Nanocomposites Based on Conducting Polymers and Carbon Nanotubes: From Fancy Materials to Functional Applications. *J. Nanosci. Nanotechnol.* **6**, 289–302 (2006).
6. Konyushenko, E. N. *et al.* Multi-wall carbon nanotubes coated with polyaniline. *Polymer* **47**, 5715–5723 (2006).
7. Antiohos, D. *et al.* Compositional effects of PEDOT-PSS/single walled carbon nanotube films on supercapacitor device performance. *J. Mater. Chem.* **21**, 15987–15994 (2011).
8. Fan, H., Wang, H., Zhao, N., Zhang, X. & Xu, J. Hierarchical nanocomposite of polyaniline nanorods grown on the surface of carbon nanotubes for high-performance supercapacitor electrode. *J. Mater. Chem.* **22**, 2774–2780 (2012).
9. Hernandez, Y. R. *et al.* Comparison of carbon nanotubes and nanodisks as percolative fillers in electrically conductive composites. *Scripta Mater.* **58**, 69–72 (2008).
10. Kilbride, B. E. *et al.* Experimental observation of scaling laws for alternating current and direct current conductivity in polymer-carbon nanotube composite thin films. *J. Appl. Phys.* **92**, 4024–4030 (2002).
11. Jalili, R., Razal, J. M. & Wallace, G. G. Exploiting high quality PEDOT:PSS-SWNT composite formulations for wet-spinning multifunctional fibers. *J. Mater. Chem.* **22**, 25174–25182 (2012).
12. Spinks, G. M., Mottaghtalab, V., Bahrami-Samani, M., Whitten, P. G. & Wallace, G. G. Carbon-Nanotube-Reinforced Polyaniline Fibers for High-Strength Artificial Muscles. *Adv. Mater.* **18**, 637–640 (2006).
13. Foroughi, J., Spinks, G. M. & Wallace, G. G. A reactive wet spinning approach to polypyrrole fibres. *J. Mater. Chem.* **21**, 6421–6426 (2011).
14. Mottaghtalab, V., Spinks, G. M. & Wallace, G. G. The development and characterisation of polyaniline-single walled carbon nanotube composite fibres using 2-acrylamido-2 methyl-1-propane sulfonic acid (AMPSA) through one step wet spinning process. *Polymer* **47**, 4996–5002 (2006).
15. Jalili, R., Razal, J. M., Innis, P. C. & Wallace, G. G. One-Step Wet-Spinning Process of Poly(3,4-ethylenedioxythiophene):Poly(styrenesulfonate) Fibers and the Origin of Higher Electrical Conductivity. *Adv. Funct. Mater.* **21**, 3363–3370 (2011).
16. Okuzaki, H., Harashina, Y. & Yan, H. Highly conductive PEDOT/PSS microfibers fabricated by wet-spinning and dip-treatment in ethylene glycol. *Eur. Polym. J.* **45**, 256–261 (2009).
17. Esrafilzadeh, D., Razal, J. M., Moulton, S. E., Stewart, E. M. & Wallace, G. G. Multifunctional conducting fibres with electrically controlled release of ciprofloxacin. *J. Control. Release* **169**, 313–320 (2013).
18. Cathcart, H. & Coleman, J. N. Quantitative comparison of ultracentrifuged and diluted single walled nanotube dispersions; differences in dispersion quality. *Chem. Phys. Lett.* **474**, 122–126 (2009).
19. Blighe, F. M. *et al.* The Effect of Nanotube Content and Orientation on the Mechanical Properties of Polymer-Nanotube Composite Fibers: Separating Intrinsic Reinforcement from Orientational Effects. *Adv. Funct. Mater.* **21**, 364–371 (2011).
20. Amiran, J. *et al.* High Quality Dispersions of Functionalized Single Walled Nanotubes at High Concentration. *J. Phys. Chem. C* **112**, 3519–3524 (2008).
21. Jonathan, N. C. Liquid-Phase Exfoliation of Nanotubes and Graphene. *Adv. Funct. Mater.* **19**, 3680–3695 (2009).
22. Coleman, J. N., Khan, U. & Gun'ko, Y. K. Mechanical Reinforcement of Polymers Using Carbon Nanotubes. *Adv. Mater.* **18**, 689–706 (2006).
23. Michele, T. B. & Yurii, K. G. Recent Advances in Research on Carbon Nanotube-Polymer Composites. *Adv. Mater.* **22**, 1672–1688 (2009).



24. Okuzaki, H., Suzuki, H. & Ito, T. Electrically driven PEDOT/PSS actuators. *Synt. Met.* **159**, 2233–2236 (2009).
25. Nikolou, M. & Malliaras, G. G. Applications of poly(3,4-ethylenedioxythiophene) doped with poly(styrene sulfonic acid) transistors in chemical and biological sensors. *Chem Rec* **8**, 13–22 (2008).
26. Ikushima, K., John, S., Ono, A. & Nagamitsu, S. PEDOT/PSS bending actuators for autofocus micro lens applications. *Synt. Met.* **160**, 1877–1883 (2010).
27. Kirchmeyer, S. & Reuter, K. Scientific importance, properties and growing applications of poly(3,4-ethylenedioxythiophene). *J. Mater. Chem.* **15**, 2077–2088 (2005).
28. Moulton, S. E., Higgins, M. J., Kapsa, R. M. I. & Wallace, G. G. Organic Bionics: A New Dimension in Neural Communications. *Adv. Funct. Mater.* **22**, 2003–2014 (2012).
29. Asplund, M. *et al.* Toxicity evaluation of PEDOT/biomolecular composites intended for neural communication electrodes. *Biomedical Materials* **4**, 045009 (2009).
30. Naficy, S., Razal, J. M., Spinks, G. M., Wallace, G. G. & Whitten, P. G. Electrically Conductive, Tough Hydrogels with pH Sensitivity. *Chemistry of Materials* **24**, 3425–3433 (2012).
31. Abidian, M. R. *et al.* Hybrid Conducting Polymer–Hydrogel Conduits for Axonal Growth and Neural Tissue Engineering. *Adv. Healthcare Mater.* **1**, 762–767 (2012).
32. Mire, C. A., Agrawal, A., Wallace, G. G., Calvert, P. & in het Panhuis, M. Inkjet and extrusion printing of conducting poly(3,4-ethylenedioxythiophene) tracks on and embedded in biopolymer materials. *J. Mater. Chem.* **21**, 2671–2678 (2011).
33. Coleman, J. N., Khan, U., Blau, W. J. & Gun'ko, Y. K. Small but strong: A review of the mechanical properties of carbon nanotube-polymer composites. *Carbon* **44**, 1624–1652 (2006).
34. Blond, D., McCarthy, D. N., Blau, W. J. & Coleman, J. N. Toughening of Artificial Silk by Incorporation of Carbon Nanotubes. *Biomacromolecules* **8**, 3973–3976 (2007).
35. Dalton, A. B. *et al.* Super-tough carbon-nanotube fibres. *Nature* **423**, 703–703 (2003).
36. Kumar, S. *et al.* Synthesis, Structure, and Properties of PBO/SWNT Composites. *Macromolecules* **35**, 9039–9043 (2002).
37. Zhang, X. *et al.* Gel spinning of PVA/SWNT composite fiber. *Polymer* **45**, 8801–8807 (2004).
38. Cooper, C. A., Young, R. J. & Halsall, M. Investigation into the deformation of carbon nanotubes and their composites through the use of Raman spectroscopy. *Composites Part A* **32**, 401–411 (2001).
39. Barisci, J. N. *et al.* Properties of Carbon Nanotube Fibers Spun from DNA-Stabilized Dispersions. *Adv. Funct. Mater.* **14**, 133–138 (2004).
40. Kozlov, M. E. *et al.* Spinning Solid and Hollow Polymer-Free Carbon Nanotube Fibers. *Adv. Mater.* **17**, 614–617 (2005).
41. Zhang, M., Atkinson, K. R. & Baughman, R. H. Multifunctional Carbon Nanotube Yarns by Downsizing an Ancient Technology. *Science* **306**, 1358–1361 (2004).
42. Zhang, X. *et al.* Strong Carbon-Nanotube Fibers Spun from Long Carbon-Nanotube Arrays. *Small* **3**, 244–248 (2007).
43. Razal, J. M., Gilmore, K. J. & Wallace, G. G. Carbon Nanotube Biofiber Formation in a Polymer-Free Coagulation Bath. *Adv. Funct. Mater.* **18**, 61–66 (2008).
44. Frackowiak, E., Khomenko, V., Jurewicz, K., Lota, K. & Béguin, F. Supercapacitors based on conducting polymers/nanotubes composites. *J. Power Sources* **153**, 413–418 (2006).
45. Snook, G. A., Kao, P. & Best, A. S. Conducting-polymer-based supercapacitor devices and electrodes. *J. Power Sources* **196**, 1–12 (2011).

## Acknowledgments

The authors thank the Australian Research Council (ARC) for financial support and the Australian National Fabrication Facility (ANFF) Materials Node for their provision of research facilities. This work was supported by ARC Federation Fellowship (GGW). J.M.R. acknowledges financial support from UOW, ARC and AIIM.

## Author contributions

R.J., J.M.R. and G.G.W. initiated the idea. R.J. carried out the experiments and interpreted the data with J.M.R. Figures were prepared by R.J. R.J. and J.M.R. wrote the main manuscript text. All authors reviewed the manuscript.

## Additional information

Supplementary information accompanies this paper at <http://www.nature.com/scientificreports>

**Competing financial interests:** The authors declare no competing financial interests.

**How to cite this article:** Jalili, R., Razal, J.M. & Wallace, G.G. Wet-spinning of PEDOT:PSS/Functionalized-SWNTs Composite: a Facile Route Toward Production of Strong and Highly Conducting Multifunctional Fibers. *Sci. Rep.* **3**, 3438; DOI:10.1038/srep03438 (2013).



This work is licensed under a Creative Commons Attribution-NonCommercial-NoDerivs 3.0 Unported license. To view a copy of this license, visit <http://creativecommons.org/licenses/by-nc-nd/3.0>